Breaking the Phonon Bottleneck in PbSe and CdSe Quantum Dots: Time-Domain Density Functional Theory of Charge Carrier Relaxation

ARTICLE *in* ACS NANO · FEBRUARY 2009

Impact Factor: 12.88 · DOI: 10.1021/nn800674n · Source: PubMed

3 AUTHORS:

Svetlana Kilina
North Dakota State University
62 PUBLICATIONS **1,395** CITATIONS
SEE PROFILE

Dmitri Kilin
University of South Dakota
85 PUBLICATIONS **871** CITATIONS
SEE PROFILE

Oleg Prezhdo
University of Rochester
306 PUBLICATIONS **6,766** CITATIONS
SEE PROFILE

Breaking the Phonon Bottleneck in PbSe and CdSe Quantum Dots: Time-Domain Density Functional Theory of Charge Carrier Relaxation

Svetlana V. Kilina, Dmitri S. Kilin, and Oleg V. Prezhdo*

Department of Chemistry, University of Washington, Seattle, Washington 98195-1700

ABSTRACT Spatial confinement can create relaxation bottlenecks by mismatch between electronic and vibrational frequencies. This hypothesis motivated discovery of multiple excitons, which could greatly enhance the efficiency of quantum dot (QD) solar cells. Surprisingly, recent experiments showed no bottleneck. Our time-domain *ab initio* study of the electron−phonon dynamics rationalizes the fast relaxation in PbSe and CdSe QDs, which have substantially different electronic properties. Atom fluctuations and surface effects lift degeneracies and create dense distributions of electronic levels at all but the lowest energies, while confinement enhances the electron−phonon coupling. The analysis applies to nanomaterials in general, modifying the fundamental view on the electron−phonon interaction.

KEYWORDS: quantum dots · electron−phonon relaxation · time-domain density functional theory · multiple excitons · solar cells

Confinement of charge carriers in quantum dots (QDs) of sizes smaller or similar to the Bohr exciton radius dictates the QD size-tunable electronic properties and makes them a promising material for various applications, ranging from opto-electronic devices, such as solar cells,[1−7] light-emitting diodes,[8] field-effect transistors,[9,10] and lasers,[11] to quantum computing[12] and biological imaging probes.[13] The electron−phonon interaction plays key roles in most of these applications and carries significant fundamental importance. Although the phonon-mediated relaxation of electrons and holes in QDs is the focus of many experimental[1,14−17] and theoretical[18,19] efforts, the fundamental understanding of the problem is not yet satisfactory, and a number of controversies remain unresolved. In particular, quantization of the electronic energy levels induced in the QDs by spatial confinement[20] and resulting in a mismatch between the electronic gaps and phonon frequencies has led to the expectation of a dramatic slowing down of the electron−phonon relaxation, known as the phonon bottleneck.[1] The spacing between the electronic levels is clearly seen in the optical spectra.[21] Unexpectedly, the recent time-resolved experiments showed picosecond relaxation, similarly to that observed in bulk.[14−17] Moreover, the relaxation rates increased with decreasing QD size, even though the electronic energy spacing became larger.[15]

The fundamental study of the phonon bottleneck question is strongly motivated by its practical significance. For example, in a gain medium based on QDs, it is desirable that excited carriers relax rapidly to their lowest states, from which radiative recombination occurs.[22] Therefore, a phonon bottleneck would be likely to hinder the operation of lasers and other light-emitting devices. On the contrary, by slowing down the decay of the electronic energy, a phonon bottleneck in photovoltaic QD materials would favor charge carrier multiplication, which carries great promise for increased efficiencies of QD solar cells.[1,3−6] The experimentally observed fast carrier relaxation at high excitation energies creates an additional puzzle regarding the mechanism of the carrier multiplication that occurs in spite of the fast energy loss.[1,3,23,24]

Here, we use state-of-the-art time-domain (TD) *ab initio* density functional theory (DFT)[25] in order to study the charge-phonon relaxation dynamics in PbSe and CdSe QDs, which represent two widely used semiconductors with substantially different electronic structure. We show at the atomistic level that the subpicosecond relaxation and the absence of the phonon bottleneck in both materials are due to efficient nonadiabatic (NA) decay channels. A dense distribution of electron and hole states arises at all but the lowest excitation energies due

*Address correspondence to prezhdo@u.washington.edu.

Received for review September 27, 2008 and accepted December 15, 2008.

Published online December 30, 2008.
10.1021/nn800674n CCC: $40.75

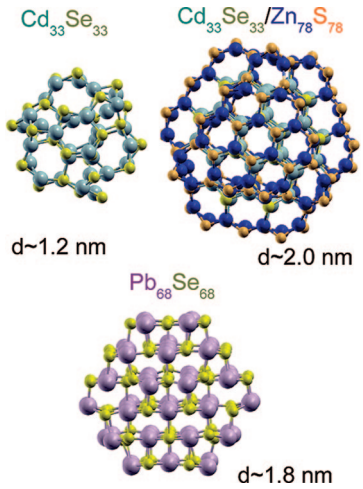

Figure 1. Optimized geometric structures of the $Cd_{33}Se_{33}$, core/shell $Cd_{33}Se_{33}/Zn_{78}S_{78}$, and $Pb_{68}Se_{68}$ QDs.

to lifting of the ideal state degeneracy by thermal fluctuations in the QD atomic structure and surface reorganization. While many states show weak optical activity, creating a discrete electronic spectrum, most of the states participate in the electron-vibrational relaxation. Similarly to molecular systems, the spatial confinement creates strong electron−phonon coupling. Even though the multiphonon processes previously proposed based on the temperature dependence of experimental relaxation rates[1,14,26] do take place in our simulations, they are not required at the higher energies due to the large density of states (DOS). The reported results apply generally to nanoscale systems and alter the commonly accepted view regarding the effect of quantum confinement on the electron−phonon relaxation dynamics.

RESULTS AND DISCUSSION

The PbSe and CdSe QDs used in the present study are shown in Figure 1. The QD geometries were generated from bulk and fully optimized at zero temperature. The $Cd_{33}Se_{33}$ and $Pb_{68}Se_{68}$ clusters used in the TD simulations are 1.3 and 1.8 nm in diameter, respectively. In order to elucidate the effects of surface reconstruction and the outer-shell layer on the QD electronic structure, a core−shell CdSe/ZnS QD was built and compared to the pure CdSe QD. Introduction of the shell-layer in the $Cd_{33}Se_{33}/Zn_{78}S_{78}$ cluster increased the diameter from 1.3 to 2 nm.

Electronic Structure of the Quantum Dots. The DOS of the CdSe, CdSe/ZnS, and PbSe QDs are shown in the insets of Figure 2. The electronic energy levels calculated for the QD geometries at 0 K were broadened in order to account for thermal atomic motions. The energy fluctuations were computed along the MD trajectory. The calculated variances on the order of 50−100 meV were used to broaden the levels. The first peak in the conduction band (CB) is clearly seen in both CdSe and PbSe QDs and is attributed in the effective-mass representation[1] to the S-electron state. This state has roughly spherically symmetric charge density distribution, which is delocalized over the whole dot, and originates from the s-type atomic orbitals of Se atoms. The higher energy peaks can be attributed to the P, D, *etc.* electronic levels of the QDs, although the state symmetry becomes harder to discern by looking at the state densities obtained in the atomistic simulation. The corresponding state structure in the valence band (VB) is less pronounced since the states are closer in energy. This agrees with the effective-mass theory, which uses a higher effective mass for holes than for electrons.

Although the calculated DOS does show distinct peaks, the peaks are well separated only at the lowest energies (Figure 2). This feature is a key in explaining the observed and simulated ultrafast charge-phonon relaxation dynamics. In its most straightforward formulation, the effective-mass description predicts that the electronic energy levels are highly degenerate. The atomistic simulation shows that the underlying atomic structure, surface effects, core/shell interactions, thermal fluctuations, as well as the spin−orbit and Coulomb coupling, break the degeneracy and create a complicated multilevel electronic structure. The existence of multiple non-degenerate energy levels near the band edge does not contradict the experimental data. Thus, significant homogeneous broadening and a complex structure of fluorescence spectra seen in single PbS QDs[27] may be a sign for the degeneracy breaking of the lowest energy electronic transition. Further, the observed photoluminescence blinking in single CdSe[28] and PbS[27] QDs demonstrates a highly non-exponential

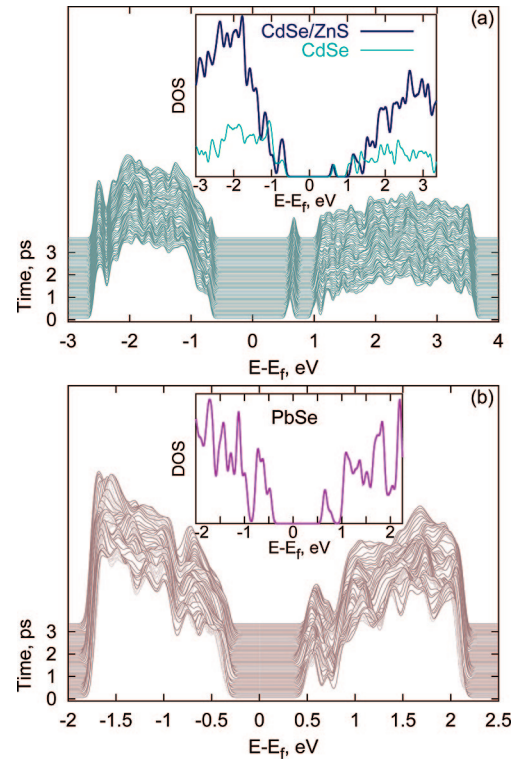

Figure 2. Densities of the electron and hole states in (a) $Cd_{33}Se_{33}$ and (b) $Pb_{68}Se_{68}$ QDs as functions of time along room-temperature MD trajectories. The CdSe DOS shows a more pronounced asymmetry across the band gap than the PbSe DOS, with the hole states having a higher density. The insets represent the DOS computed for the perfectly optimized dot geometry and broadened by the energy fluctuations from the MD simulations. The $Cd_{33}Se_{33}$ DOS agrees with the DOS of the core/shell $Cd_{33}Se_{33}/Zn_{78}S_{78}$ QD, indicating that surface relaxation of $Cd_{33}Se_{33}$ eliminates gap states, which could have been expected due to surface dangling bonds.

decay of the probability density for a given on or off time. This observation may indicate that the photogenerated exciton is not transitioning between a single bright state (on) and a single dark state (off) but is distributed over multiple on/off states.

Surface passivation by an inorganic shell or organic ligands may be expected to change dramatically the QD DOS. In order to test this possibility, we compare the DOS of the $Cd_{33}Se_{33}$ QD and the core/shell $Cd_{33}Se_{33}/Zn_{78}S_{78}$ dot in the inset of Figure 2a. If QDs had preserved the ideal bulk structure, the multiple unsaturated chemical bonds on the surface would have introduced band gap states, drastically reducing the gap. Reference 29 shows that surface relaxation can eliminate gap states under the condition that surface atoms have no more than one dangling bond. Our calculation reproduces this effect and shows further that the surface reconstruction and the band gap is maintained when temperature is raised to 300 K; compare the main panels and the insets in Figure 2. The surface reconstruction is quite subtle in our case and preserves the wurtzite and zinc blende topologies of bulk CdSe and PbSe, respectively, at both 0 and 300 K. Quite remarkably, the surface relaxation is nearly equivalent to the presence of a shell layer; see the inset in Figure 2a. Because ZnS has a much larger band gap than CdSe, the band edge states of the core/shell structure originate from the CdSe core, and the DOS of the CdSe and CdSe/ZnS QDs differ significantly only at higher energies. PbSe is much less susceptible to surface effects when compared to CdSe.[30] Therefore, the similarity between the core/shell and bare-core DOS near the band edge should be valid not only for CdSe but also for PbSe. The extensive computation effort limited the NA TDDFT simulations to the pure CdSe and PbSe clusters, which are shown in Figure 1.

The calculated zero temperature energy gaps are 1.58 eV for the $Cd_{33}Se_{33}$, 1.59 eV for the core−shell CdSe/ZnS, and 1.15 eV for the PbSe. These values are underestimated relative to experiment,[28] as is typical with DFT calculations that use density or density gradient functionals, such as PW91 employed here. This problem is attributed to incomplete elimination of the self-interaction energy by these functionals.[31,32] Long-range non-local and non-adiabatic corrections are routinely used to remedy the problem, for instance, in hybrid functionals that include a portion of the exact Hartree−Fock exchange. Hybrid functionals consistently provide energy gaps that are close to the experimental values.[33,34] However, hybrid functionals require additional computational efforts, and their utilization in the NA TDDFT simulations is problematic. On the other hand, in contrast to the studies of non-radiative fluorescence quenching,[35] the absolute values of the energy gaps are not relevant for the present investigation. Our focus is on the intraband NA dynamics, which involve electron and hole relaxation inside the bands, rather than across the band gap. The results of these dynamics depend on accurate calculations of energy levels in the QD VB and CB, which are typically well reproduced by functionals that are based on density and density gradient.

The calculated PbSe DOS is notably more symmetric than the CdSe DOS, as expected.[15] This is seen particularly well with the heights of the peaks in Figure 2. The VB peaks are higher than the CB peaks in CdSe, while they have similar heights in PbSe. As predicted by the effective-mass theory,[1] the CdSe holes are several times heavier than electrons. Although the PbSe holes do show a slightly higher DOS than electrons, this asymmetry is much less pronounced than in CdSe. Compared to the effective-mass and tight-binding calculations, our *ab initio* results demonstrate more complex electronic structure for both PbSe and CdSe QDs, in agreement with the recent atomistic pseudopotential calculations.[36]

The asymmetry of the DOS of the CdSe QD favors the Auger relaxation channel, by which the electron exchanges its excitation energy with the hole, and the hole relaxes fast through its denser manifold of states by the NA coupling to phonons.[16] The Auger process is considered to be the main channel of the fast non-radiative relaxation of electrons in CdSe QDs.[37] However, the Auger relaxation can be efficient only when the photoexcited electrons and holes are coupled *via* the Coulomb interaction. The time-resolved experiments in CdSe QDs show that the intraband relaxation is fast even if the holes are decoupled from the electrons either through the hole trapping at the surface and ligands[38] or *via* electron injection into neutral dots with no holes.[39] Consequently, mechanisms other than the Auger scattering lead to the fast relaxation of the decoupled carriers. The NA relaxation of the electrons and holes studied in the present work is the most probable scenario for the above cases.

The evolution of the DOS induced by thermal atomic motions is shown in the main panels of Figure 2. The DOS is plotted along the *z*-axis as a function of energy and time. The CB and VB edge energies change by less than 0.1 eV. The edge of the VB in both dots is significantly smoothed by the thermal motion. The gaps between the S and P states of the holes disappear, and the states mix when the temperature is raised. The electronic S states remain separated from the rest of the CB manifold in both QDs, particularly in the smaller CdSe cluster.

Non-adiabatic Relaxation of Photoexcited Charge Carriers. The initially populated states are chosen to satisfy simultaneously the following three conditions. First, the transition energies are chosen to be roughly three times the QD energy gap. Second, by computing the transition dipole moment, specific electron−hole excitations are selected within this energy range to have the largest optical activity. Third, only those transitions that are

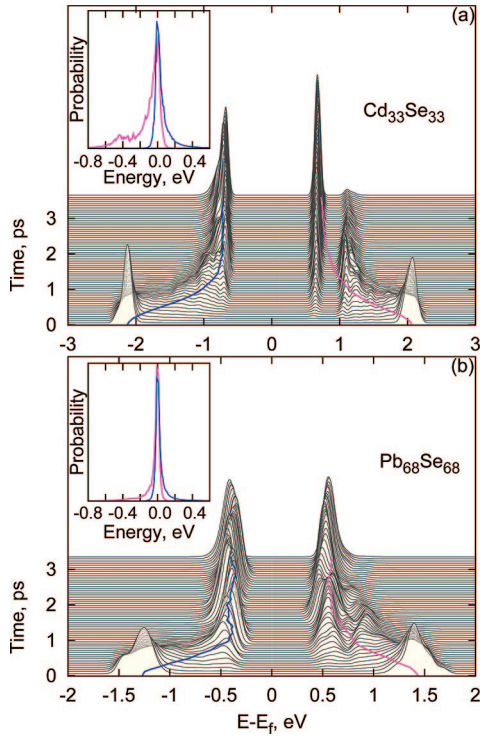

Figure 3. Relaxation of the electron (blue lines) and hole (magenta lines) energies in (a) $Cd_{33}Se_{33}$ and (b) $Pb_{68}Se_{68}$. The plots are obtained by multiplying the DOS, Figure 2, by the corresponding state occupations and averaging over 500 initial conditions. The major part of the relaxation occurs within the first picosecond and is highly non-exponential. A slower relaxation component associated with the relaxation all the way to the band gap states occurs on a slower time scale, as seen particularly well with the gradual growth of the lowest electron state population in CdSe. Insets: Probability density for the electron (blue) and hole (magenta) transitions as a function of the transition energy. Both resonant and multiphonon processes are seen, since the energy exchanged during a transition is often greater than the characteristic phonon energy of 0.025 eV. The multiphonon relaxation is most pronounced for the electrons in $Cd_{33}Se_{33}$.

roughly symmetric around the center of the band gap are considered. These three requirements satisfy the experimental conditions for the PbSe QDs,[5] in which the carriers have nearly the same effective masses, and the CB and VB structures are almost symmetric. In the case of CdSe QDs, holes are significantly heavier than electrons, and the last provision is not required. Transitions between high energy electrons and low energy holes and *vice versa* are also optically allowed.[38] For comparison, we use the same three requirements for selecting the initial photoexcitations in both types of QDs.

Figure 3 presents the simulated NA dynamics of the electron and hole relaxation mediated by coupling to phonons. The three-dimensional plots are similar to those of Figure 2: the DOS plotted in Figure 2 is multiplied in Figure 3 by the evolving state occupations, representing changes in the orbital populations with respect to the ground state. As evidenced by the data, the charge carriers visit multiple states during the relaxation, and none of the intermediate states play a special role. The non-equilibrium population peaks created by the photoexcitation spread to reappear near the band gap. The main part of the relaxation, that is, when most of states near the band gap are populated, is complete within a picosecond. This relaxation time agrees well with the experimental data.[14−17]

The observed relaxation dynamics is highly non-exponential (see the blue and magenta lines in Figure 3), in agreement with the strongly non-Lorentzian line shapes observed experimentally.[27] The electron and hole energy loss in both CdSe and PbSe QDs is dominated by a Gaussian component at small times. The non-exponential decay seen in our time-domain calculation cannot be obtained using perturbation theory, such as the Fermi Golden Rule, which provides exponential relaxation rates. The relaxation rate computed in our approach varies with time and exhibits memory effects. In general, Gaussian relaxation occurs by a coherent quantum-mechanical process. Such a process, for example, gives rise to the quantum Zeno effect, associated with the vanishing time derivative of the quantum-mechanical transition probability at zero time.[40] The incoherent exponential component becomes important at lower energies for the electrons and at higher energies for the holes. There, closer to the band gap, the energy spacings between the states become larger, and quantum transitions take longer than pure dephasing.[41] The transitions deep inside the VB and CB occur faster than pure dephasing. This is possible because the majority of the states present in the DOS within the relevant energy range participate in the electron−phonon relaxation.

No phonon bottleneck is observed, except at the last stage of the electron relaxation in the CdSe QD, which exhibits two distinct population peaks even after 3.5 ps (Figure 3a). This case shows that a bottleneck is indeed possible if the energy gaps between the electronic states are larger than the phonon frequencies.[1] In the CdSe QD, the S-electron level remains well-separated from the rest of the CB manifold by an energy gap of around 0.3 eV because of the small size of the dot. The pure dephasing time[41] in this case is shorter than the transition time. Therefore, applied to this transition, the current computational technique has to be augmented for the loss of coherence, as has been done in the recent study of non-radiative fluorescence quenching in carbon nanotubes.[35] The analysis performed in ref 35 suggests that loss of quantum coherence can significantly slow down the final stage of the simulated relaxation compared to the current result. This expectation is closely related to the quantum Zeno effect.[40] Further study of the final stage of the electron relaxation in the CdSe QD is currently underway, motivated by the recent experimental data.[42]

In the larger PbSe QD, the final CB peak spreads over several dense states at the band edge, and the relaxation is fully complete by the end of the run show-

ing no phonon bottleneck. Analogously, the holes in both materials completely populate several VB states at the band edge by the end of the simulation time of 3.5 ps. The populations of the final states close to the band edge are distributed according to the Boltzmann distribution. In the CdSe QD, the photoexcited electrons relax notably slower than the holes. This agrees with the experiments, in which the Auger exchange of energy between electrons and holes have been suppressed by hole trapping,[38] and in which the electrons were injected into the dots.[39]

The insets in Figure 3 give the normalized probability densities for the electron and hole transitions as a function of the transition energy. The transitions can occur both up and down in energy; however, transitions downward dominate, as required by the detailed balance.[43] The most likely transitions involve small amounts of energy that are close to the phonon energy on the order of 100−200 cm^{-1} (12−25 meV). This fact indicates that the energy gaps between the electronic states are very small, especially at the higher excitation energies, explaining the absence of the phonon bottleneck. Occasionally, up to 0.3−0.6 eV of electronic energy can be lost to phonons in a single event. This happens more often with electrons than holes, at lower energies and in the smaller CdSe QDs. Transitions that exchange large amounts of energy between the electronic and vibrational degrees of freedom involve multiple phonon quanta. Thus, the multiphonon relaxation mechanism proposed initially in order to rationalize the ultrafast experimental data[14,15] is indeed seen in our simulation; however, the faster resonant electron−phonon energy exchange is more efficient, particularly in the higher energy range.

CONCLUSIONS

In summary, our time-domain *ab initio* study of the electron−phonon relaxation dynamics in the CdSe and PbSe QDs rationalized the controversy between the theoretical prediction of the electron−phonon relaxation bottleneck and the experimental lack thereof. The relaxation is fast because the underlying atomic structure, surface reconstruction, thermal fluctuations, and other factors break the perfect symmetry of the QDs, lift electronic state degeneracies, and generate a dense distribution of energy levels. The conclusion applies not only to the CdSe and PbSe QDs studied here, but also to other nanoscale systems, including carbon nanotubes[44] and chromophore−semiconductor interfaces.[25,45]

The electron−phonon relaxation can be both resonant and multiphonon. At higher energies, the spacing between the electronic levels is on the order of the phonon frequencies, allowing the resonant energy exchange. At energies close to the band gap, the relaxation takes place by the multiphonon mechanism, and a signature of the phonon bottleneck is seen. The transfer of the excess electron and hole energies to phonons is coherent and non-exponential at the higher energies. The NA electronic transitions are faster than loss of the quantum phase information.

The calculations show that reconstruction of the QD surface efficiently accommodates surface dangling bonds and produces the same band gap as the core/shell QD design, in which the dangling bonds of the core are passivated by chemical interactions with the shell.

The details provided by our state-of-the-art simulations contribute to the unified picture of the relaxation dynamics in semiconductor QDs, by altering and expanding the commonly accepted view on the role of quantum confinement in the electron−phonon interaction.

METHODS

The time-domain *ab initio* simulation of the electron−phonon relaxation dynamics is based on the implementation[25] of the fewest switching surface hopping (FSSH) technique[43,46,47] within time-domain Kohn−Sham (TDKS) theory.[48] FSSH is an atomistic non-adiabatic molecular dynamics approach that satisfies detailed balance[43] and, therefore, can be used to study relaxation processes and decay to thermodynamic equilibrium. FSSH can be viewed as a quantum master equation, in which the state-to-state electronic transition rates depend on time through coupling to phonon dynamics.

The TDKS−FSSH theory was implemented within the VASP package.[49] The simulations were performed with the Perdew and Wang exchange-correlation functional[50] and Vanderbilt pseudopotentials.[51] A converged plane-wave basis was used in cubic simulation cells periodically replicated in three dimensions. In order to prevent spurious interactions between periodic images of the QDs, the cells were constructed to have at least 8 Å of vacuum between the QD replicas.

The PbSe and CdSe QDs were initially constructed to have the structure of the bulk semiconductors. Then, the QDs were relaxed to their lowest energy configurations. The relaxed configurations were heated to 300 K by repeated velocity rescaling and used for the dynamics calculations. Five picosecond microcanonical trajectories were generated in the ground electronic state. Five hundred random initial conditions were sampled from these trajectories in order to create an ensemble of photoexcited QDs for the NA dynamics. A 2 fs nuclear and a 10^{-3} fs electronic time step were used for the dynamics calculations.

The two components of the TDKS−FSSH methodology are outlined below. Further details can be found in refs 19, 25, 35, 44, 45.

Time-Domain Kohn−Sham Theory. The electron density is written in the KS representation[48] as

$$\rho(x,t) = \sum_{p=1}^{N_e} |\varphi_p(x,t)|^2 \qquad (1)$$

where N_e is the number of electrons and the $\varphi_p(x,t)$ are single-electron KS orbitals. The evolution of $\varphi_p(x,t)$ is determined by application of the time-dependent variational principle to the expectation value of the Kohn−Sham density functional and leads to the system of coupled equations of motion for the single-particle KS orbitals[48]

$$i\hbar\frac{\partial\varphi_p(x,t)}{\partial t} = H\{\varphi(x,t)\}\varphi_p(x,t), \quad p = 1, \ldots, N_e \qquad (2)$$

The equations are coupled since the Hamiltonian H depends on the density (eq 1) and, hence, all KS orbitals occupied by the N_e electrons. Expanding the time-dependent KS orbitals $\varphi_p(x, t)$ in the adiabatic KS orbitals $\varphi_k(x; R)$

$$\varphi_p(x, t) = \sum_k^{N_e} c_{pk}(t)|\tilde{\varphi}_k(x;R)\rangle \quad (3)$$

the TDKS eq 2 transforms to the equation of motion for the expansion coefficients

$$i\hbar\frac{\partial}{\partial t}c_{pk}(t) = \sum_m^{N_e} c_{pm}(t)(\varepsilon_m\delta_{km} + \mathbf{d}_{km}\cdot\dot{\mathbf{R}}) \quad (4)$$

The adiabatic KS orbitals are obtained by solving the time-independent KS equations, which are implemented in many computer codes. We use VASP.[49] The non-adiabatic coupling

$$\mathbf{d}_{km}\cdot\dot{\mathbf{R}} = -i\hbar\langle\tilde{\varphi}_k(x;R)|\nabla_{\mathbf{R}}|\tilde{\varphi}_m(x;R)\rangle\cdot\dot{\mathbf{R}} = -i\hbar\langle\tilde{\varphi}_k|\frac{\partial}{\partial t}|\tilde{\varphi}_m\rangle \quad (5)$$

arises from the dependence of the adiabatic KS orbitals on the phonon dynamics, and is computed numerically according to the right-hand-side of eq 5.[47] The prescription for phonon dynamics $\mathbf{R}(t)$ constitutes the quantum backreaction problem. In order to define the backreaction, FSSH uses a stochastic algorithm that generates trajectory branching[46] and detailed balance.[43] Trajectory branching mimics the splitting of quantum mechanical wavepackets describing phonons in correlation with different electronic states. Detailed balance ensures that transitions up in energy are less likely than transitions down in energy by the Boltzmann factor. It is essential for studying electron−phonon relaxation and achieving thermodynamic equilibrium.

Fewest Switches Surface Hopping. FSSH requires an electronic basis. Preferably, the basis is formed of adiabatic states.[43,46,47] While the adiabatic forces for the ground and excited electronic states as well as the NA coupling between them can be calculated in TDDFT,[48] the NA coupling between excited electronic states remains an open question.[52] We use the zeroth-order adiabatic basis formed of the adibatic KS orbitals. Compared to the original implementation of the TDKS-FSSH method,[25] we use a further approximation by going from the many-particle Slater determinant basis to the single-particle representation. The FSSH simulation is performed separately for electrons and holes in the basis of single-particle adiabatic KS orbitals. The single-particle representation is appropriate for studies of QDs since their electronic structure is well represented by the independent electron and hole picture. Quantum confinement effects in QDs ensures that the electron and hole kinetic energies dominate the electrostatic interaction. As a result, even the basic effective mass theory provides a good description of the QD electronic structure.[37]

FSSH prescribes a probability for hopping between electronic states. The probability is explicitly time-dependent and is correlated with the nuclear evolution. Specifically,[46] the probability of a hop between states k and m within the time interval dt equals to

$$dP_{km} = \frac{b_{km}}{a_{kk}}dt \quad (6)$$

where

$$b_{km} = -2\mathrm{Re}(a_{km}^*\mathbf{d}_{km}\cdot\dot{\mathbf{R}});\ a_{km} = c_k c_m^* \quad (7)$$

Here, c_k and c_m are the coefficients evolving according to eq 4. The hopping probabilities explicitly depend on the NA coupling $\mathbf{d}_{km}\cdot\dot{\mathbf{R}}$ defined in eq 5. If the calculated dP_{km} is negative, the hopping probability is set to zero. This feature minimizes the number of hops: a hop from state k to state m can occur only when the electronic occupation of state k decreases and the occupation of state m increases. To conserve the total electron−nuclear energy after a hop, the original FSSH technique rescales the nuclear velocities along the direction of the electronic component $\mathbf{d}_{km}$ of the NA coupling.[46,47] If a NA transition to a higher energy electronic state is predicted by eq 6, and the kinetic energy available in the nuclear coordinates along the direction of the NA coupling is insufficient to accommodate the increase in the electronic energy, the hop is rejected. The velocity rescaling and hop rejection give detailed balance between upward and downward transitions.[43]

The current, simplified implementation of FSSH makes the assumption that the energy exchanged between the electronic and nuclear degrees of freedom during the hop is rapidly redistributed between all nuclear modes. With this assumption, the distribution of energy in the nuclear modes is Boltzmann at all times, and the velocity rescaling/hop rejection step can be replaced by multiplying the probability (eq 6) for transitions upward in energy by the Boltzmann factor. This simplification of the original FSSH technique gives great computational savings, allowing us to determine the TD potential that drives the dynamics of the electronic subsystem using the ground-state trajectory.

Acknowledgment. S.K. is grateful to Andrei Piryatinski and Kiril Tsemekhman for fruitful discussions, and to Sergei Tretiak for hosting the GRA Fellowship visit at the Los Alamos National Laboratory during manuscript preparation. The research was supported by grants from NSF CHE-0701517 and ACS-PRF 46772-AC6.

REFERENCES AND NOTES

1. Nozik, A. J. Spectroscopy and Hot Electron Relaxation Dynamics in Semiconductor Quantum Wells and Quantum Dots. *Annu. Rev. Phys. Chem.* **2001**, *52*, 193–231.
2. Koleilat, G. I.; Levina, L.; Shukla, H.; Myrskog, S. H.; Hinds, S.; Pattantyus-Abraham, A. G.; Sargent, E. H. Efficient, Stable Infrared Photovoltaics Based on Solution-Cast Colloidal Quantum Dots. *ACS Nano* **2008**, *2*, 833–840.
3. Ellingson, R. J.; Beard, M. C.; Johnson, J. C.; Yu, P.; Micic, O. I.; Nozik, A. J.; Shabaev, A.; Efros, A. L. Highly Efficient Multiple Exciton Generation in Colloidal PbSe and PbS Quantum Dots. *Nano Lett.* **2005**, *5*, 865–871.
4. Beard, M. C.; Knutsen, K. P.; Yu, P. R.; Luther, J. M.; Song, Q.; Metzger, W. K.; Ellingson, R. J.; Nozik, A. J. Multiple Exciton Generation in Colloidal Silicon Nanocrystals. *Nano Lett.* **2007**, *7*, 2506–2512.
5. Schaller, R. D.; Klimov, V. I. High Efficiency Carrier Multiplication in PbSe Nanocrystals: Implications for Solar Energy Conversion. *Phys. Rev. Lett.* **2004**, *92*, 18660-1–18660-4.
6. Schaller, R. D.; Agranovich, V. M.; Klimov, V. I. High-Efficiency Carrier Multiplication through Direct Photogeneration of Multi-Excitons *via* Virtual Single-Exciton States. *Nat. Phys.* **2005**, *1*, 189–194.
7. Kumar, S.; Jones, M.; Lo, S. S.; Scholes, G. D. Nanorod Heterostructures Showing Photoinduced Charge Separation. *Small* **2007**, *3*, 1633–1639.
8. Coe, S.; Woo, W. K.; Bawendi, M.; Bulovic, V. Electroluminescence from Single Monolayers of Nanocrystals in Molecular Organic Devices. *Nature* **2002**, *420*, 800–803.
9. Talapin, D. V.; Murray, C. B. PbSe Nanocrystal Solids for n- and p-Channel Thin Film Field-Effect Transistors. *Science* **2005**, *310*, 86–89.
10. Luther, J. M.; Law, M.; Song, Q.; Perkins, C. L.; Beard, M. C.; Nozik, A. J. Structural, Optical and Electrical Properties of Self-Assembled Films of PbSe Nanocrystals Treated with 1,2-Ethanedithiol. *ACS Nano* **2008**, *2*, 271–280.
11. Klimov, V. I.; Mikhailovsky, A. A.; Xu, S.; Malko, A.; Hollingsworth, J. A.; Leatherdale, C. A.; Eisler, H. J.; Bawendi, M. G. Optical Gain and Stimulated Emission in Nanocrystal Quantum Dots. *Science* **2000**, *290*, 314–317.
12. Petta, J. R.; Johnson, A. C.; Taylor, J. M.; Laird, E. A.; Yacoby, A.; Lukin, M. D.; Marcus, C. M.; Hanson, M. P.; Gossard, A. C.

Coherent Manipulation of Coupled Electron Spins in Semiconductor Quantum Dots. *Science* **2005**, *309*, 2180–2184.
13. Dahan, M.; Levi, S.; Luccardini, C.; Rostaing, P.; Riveau, B.; Triller, A. Diffusion Dynamics of Glycine Receptors Revealed by Single-Quantum Dot Tracking. *Science* **2003**, *302*, 442–445.
14. Schaller, R. D.; Pietryga, J. M.; Goupalov, S. V.; Petruska, M. A.; Ivanov, S. A.; Klimov, V. I. Breaking the Phonon Bottleneck in Semiconductor Nanocrystals *via* Multiphonon Emission Induced by Intrinsic Nonadiabatic Interactions. *Phys. Rev. Lett.* **2005**, *95*, 19640-1–19640-4.
15. Harbold, J. M.; Du, H.; Krauss, T. D.; Cho, K.-S.; Murray, C. B.; Wise, F. W. Time-Resolved Intraband Relaxation of Strongly Confined Electrons and Holes in Colloidal PbSe Nanocrystals. *Phys. Rev. B* **2005**, *72*, 195312-1–195312-6.
16. Cooney, R. R.; Sewall, S. L.; Anderson, K. E. H.; Dias, E. A.; Kambhampati, P. Breaking the Phonon Bottleneck for Holes in Semiconductor Quantum Dots. *Phys. Rev. Lett.* **2007**, *98*, 177403-1–177403-4.
17. Cooney, R. R.; Sewall, S. L.; Dias, E. A.; Sagar, D. M.; Anderson, K. E. H.; Kambhampati, P. Unified Picture of Electron and Hole Relaxation Pathways in Semiconductor Quantum Dots. *Phys. Rev. B* **2007**, *75*, 245311-1–245311-6.
18. Muljarov, E. A.; Takagahara, T.; Zimmermann, R. Phonon-Induced Exciton Dephasing in Quantum Dot Molecules. *Phys. Rev. Lett.* **2005**, *95*, 177405-1–177405-4.
19. Kilina, S. V.; Kilin, D. S.; Craig, C. F.; Prezhdo, O. V. *Ab Initio* Time-Domain Study of Phonon-Assisted Relaxation of Charge Carriers in a PbSe Quantum Dot. *J. Phys. Chem. C* **2007**, *111*, 4871–4878.
20. Scholes, G. D. Insights into Excitons Confined to Nanoscale Systems: Electron-Hole Interaction, Binding Energy, and Photodissociation. *ACS Nano* **2008**, *2*, 523–537.
21. Peterson, J. J.; Huang, L. B.; Delerue, C.; Allan, G.; Krauss, T. D. Uncovering Forbidden Optical Transitions in PbSe Nanocrystals. *Nano Lett.* **2007**, *7*, 3827–3831.
22. Schaller, R. D.; Petruska, M. A.; Klimov, V. I. Tunable Near-Infrared Optical Gain and Amplified Spontaneous Emission Using PbSe Nanocrystals. *J. Phys. Chem. B* **2003**, *107*, 13765–13768.
23. Franceschetti, A.; An, J. M.; Zunger, A. Impact Ionization Can Explain Carrier Multiplication in PbSe Quantum Dots. *Nano Lett.* **2006**, *6*, 2191–2195.
24. Nai, G.; Geyer, S. M.; Chang, L. Y.; Bawendi, M. G. Carrier Multiplication Yields in PbS and PbSe Nanocrystals Measured by Transient Photoluminescence. *Phys. Rev. B* **2008**, *78*, 125325-1–125325-10.
25. Craig, C. F.; Duncan, W. R.; Prezhdo, O. V. Trajectory Surface Hopping in the Time-Dependent Kohn−Sham Approach for Electron-Nuclear Dynamics. *Phys. Rev. Lett.* **2005**, *95*, 163001-1–163001-4.
26. Poddubny, A.; Goupalov, S. V. Coherent Defect-Assisted Multiphonon Intraband Carrier Relaxation in Semiconductor Quantum Dots. *Phys. Rev. B* **2008**, *77*, 075315-1–075315-7.
27. Peterson, J. J.; Krauss, T. D. Fluorescence Spectroscopy of Single Lead Sulfide Quantum Dots. *Nano Lett.* **2006**, *6*, 510–514.
28. Gooding, A. K.; Gomez, D. E.; Mulvaney, P. The Effects of Electron and Hole Injection on the Photoluminescence of CdSe/CdS/ZnS Nanocrystal Monolayers. *ACS Nano* **2008**, *2*, 669–676.
29. Yu, M.; Fernando, G. W.; Li, R.; Papadimitrakopoulos, F.; Shi, N.; Ramprasad, R. First Principles Study of CdSe Quantum Dots: Stability, Surface Unsaturations, and Experimental Validation. *Appl. Phys. Lett.* **2006**, *88*, 231910-1–231910-3.
30. Wise, F. W. Lead Salt Quantum Dots: The Limit of Strong Quantum Confinement. *Acc. Chem. Res.* **2000**, *33*, 773–780.
31. Goedecker, S.; Umrigar, C. J. Critical Assessment of the Self-Interaction-Corrected-Local-Density-Functional Method and its Algorithmic Implementation. *Phys. Rev. A* **1997**, *55*, 1765–1771.
32. Prezhdo, O. V. Assessment of Theoretical Approaches to the Evaluation of Dipole Moments of Chromophores for Nonlinear Optics. *Adv. Mater.* **2002**, *14*, 597–600.
33. Tretiak, S.; Igumenshchev, K.; Chernyak, V. Exciton Sizes of Conducting Polymers Predicted by Time-Dependent Density Functional Theory. *Phys. Rev. B* **2005**, *71*, 033201-1–033201-6.
34. Kilina, S.; Ivanov, S.; Tretiak, S. The Effect of Surface Ligands on Optical and Electronic Spectra of Semiconductor Nanoclusters. *J. Am. Chem. Soc.*, **2008**, submitted.
35. Habenicht, B. F.; Prezhdo, O. V. Nonradiative Quenching of Fluorescence in a Semiconducting Carbon Nanotube: A Time-Domain *Ab Initio* Study. *Phys. Rev. Lett.* **2008**, *100*, 197402-1–197402-4.
36. An, J. M.; Franceschetti, A.; Dudiy, S. V.; Zunger, A. The Peculiar Electronic Structure of PbSe Quantum Dots. *Nano Lett.* **2006**, *6*, 2728–2735.
37. Efros, A. L.; Kharchenko, V. A.; Rosen, M. Breaking the Phonon Bottleneck in Nanometer Quantum Dots—Role of Auger-Like Processes. *Solid State Commun.* **1995**, *93*, 281–284.
38. Klimov, V. I.; Mikhailovsky, A. A.; McBranch, D. W.; Leatherdale, C. A.; Bawendi, M. G. Mechanisms for Intraband Energy Relaxation in Semiconductor Quantum Dots: the Role of Electron-Hole Interactions. *Phys. Rev. B* **2000**, *61*, R13349–R13352.
39. Guyot-Sionnest, P.; Wehrenberg, B. L.; Yu, D. Intraband Relaxation in CdSe Nanocrystals and the Strong Influence of the Surface Ligands. *J. Chem. Phys.* **2005**, *123*, 074709-1–074709-7.
40. Prezhdo, O. V.; Rossky, P. J. Quantum Decoherence and Short Time Solvent Response. *Phys. Rev. Lett.* **1998**, *81*, 5294-1–5294-4.
41. Kamisaka, H.; Kilina, S. V.; Yamashita, Y.; Prezhdo, O. V. Ultrafast Vibrationally-Induced Dephasing of Electronic Excitations in PbSe Quantum Dots. *Nano Lett.* **2006**, *6*, 2295–2300.
42. Pandey, A.; Guyot-Sionnest, P. Slow Electron Cooling in Colloidal Quantum Dots. *Science* **2008**, *322*, 929–932.
43. Parandekar, P. V.; Tully, J. C. Mixed Quantum-Classical Equilibrium. *J. Chem. Phys.* **2005**, *122*, 094102-1–094102-6.
44. Habenicht, B. F.; Craig, C. F.; Prezhdo, O. V. Electron and Hole Relaxation Dynamics in a Semiconducting Carbon Nanotube. *Phys. Rev. Lett.* **2006**, *96*, 187401-1–187401-4.
45. Duncan, W. R.; Prezhdo, O. V. Time-Domain *Ab Initio* Study of Charge Relaxation and Recombination in Dye-Sensitized TiO_2. *J. Am. Chem. Soc.* **2007**, *129*, 8528–8543.
46. Tully, J. C. Molecular Dynamics with Electronic Transitions. *J. Chem. Phys.* **1990**, *93*, 1061–1071.
47. Hammes-Schiffer, S.; Tully, J. C. Proton Transfer in Solution: Molecular Dynamics with Quantum Transitions. *J. Chem. Phys.* **1994**, *101*, 4657–4667.
48. Marques, M. A. L.; Gross, E. K. U. Time-Dependent Density Functional Theory. *Annu. Rev. Phys. Chem.* **2004**, *55*, 427–455.
49. Kresse, G.; Furthmüller, J. Efficiency of *Ab-Initio* Total Energy Calculations for Metals and Semiconductors Using a Plane-Wave Basis Set. *Comput. Mater. Sci.* **1996**, *6*, 15–50.
50. Perdew, J. P. *Electronic Structure of Solids*; Akademie Verlag: Berlin, 1991.
51. Vanderbilt, D. Soft Self-Consistent Pseudopotentials in a Generalized Eigenvalue Formalism. *Phys. Rev. B* **1990**, *41*, 7892–7895.
52. Tapavicza, E.; Tavernelli, I.; Rothlisberger, U. Trajectory Surface Hopping within Linear Response Time-Dependent Density-Functional Theory. *Phys. Rev. Lett.* **2007**, *98*, 023001-1–023001-4.